Supplementary information for the article: Quantum algorithm for alchemical optimization in material design

Panagiotis Kl. Barkoutsos, Fotios Gkritsis, Pauline J. Ollitrault, Igor O. Sokolov, Stefan Woerner, and Ivano Tavernelli

(Dated: January 20, 2021)

Molecular Systems

For this case we consider that all molecular systems are of fixed interatomic distance. The distances between the points are recorded in Table SI-1.

TABLE SI-1. Interatomic distances for all considered molecules in vacuum. All distances are taken from ref.[1] (ref. [29] of the main text) where they were computed at CCSD(T)/cc-pVQZ level of theory.

Molecule	Distance (Å)
H_2	0.742
LiH	1.607
Li_2	2.698
LiNa	2.950
Na_2	3.177
NaH	1.926

Additional constrains on the construction of the 'alchemical' Hamiltonian can be implemented to choose certain molecular structures without further requirements in terms of quantum resources.

For the second case study we consider all possible combinations of molecules comprised by the atoms C,N,O and S. The equilibrium bond distances of the different molecules considered are summarized in Table SI-2. The orientation of the molecule is does not play a significant role, since it only has a minor effect (less than 0.1 %) on the binding energies (according to calculations executed on classical quantum chemistry drivers). To this extend we align all molecules along the z-axis, according to the atomic coordinates stated in Table SI-2.

TABLE SI-2. Interatomic distances of all heteroatomic molecules composed by the atoms in the set $\{C, N, O, S\}$. All values are in Å.

Molecule	Distance	Atom 1 & 2	Atom 1	Atom 2
		x , y	z	z
CN	1.226	17.177, 18.731	72.948	74.174
OC	1.182	17.177, 18.731	73.085	74.267
ON	1.169	17.177, 18.731	72.991	74.160
SC	1.559	17.177, 18.731	72.881	74.440
SN	1.604	17.177, 18.731	72.849	74.453
SO	1.634	17.177, 18.731	72.823	74.457

The 'alchemical' Hamiltonian

The contributions to the 'alchemical' Hamiltonian (Eq.(1) of the main text) that drives the optimization in the chemical space are:

$$K_e(r) = -\frac{\hbar^2}{2m_e}\sum_i^{N_e}\nabla_{r_i}^2 \tag{SI-1}$$

$$V_{en}(\tilde{Z}_I^{s_I}, r_i, R_I) = -\frac{e^2\,\tilde{Z}_I^{s_I}}{4\pi\epsilon_0|R_I - r_i|} \tag{SI-2}$$

$$V_{nn}(\tilde{Z}^s, R) = \sum_{I=1}^{N_n}\sum_{J>I}^{N_n}\sum_{S_I}\sum_{S_J}\alpha_{S_I}^I\alpha_{S_J}^J\frac{e^2\,\tilde{Z}_I^{s_I}\tilde{Z}_J^{s_J}}{4\pi\epsilon_0|R_I - R_J|} \tag{SI-3}$$

$$V_{ee}(r) = \sum_{i=1}^{N_e}\sum_{j>i}^{N_e}\frac{e^2}{4\pi\epsilon_0|r_i - r_j|} \tag{SI-4}$$

where ϵ_0 is the permittivity and e is the electron charge. For all atoms heavier than H we use the effective core potentials given in Table SI-3 as implemented in the Gaussian software package.[2] The calculation of the classical term in Eq.(3) scales as $N_n^2 \times N_s^2$ and therefore will never influence the scaling of the alchemical algorithm, which achieves the reduction from an exponential scaling (in the number of basis functions for the sampling of the chemical space and of the many-electron Hilbert space) to a polynomial one.

The one- and two-electron integrals in the second quantized Hamiltonian (Eq.(4) of the main text) are given by

$$h_{\mu\nu}(\tilde{Z}_I^{s_I}, R_I) = \int dr\,\phi_\mu^{AO*}(R_I, r)\left(-\frac{1}{2}\nabla_r^2 - \sum_{I=1}^{M}\frac{e^2\tilde{Z}_I^{s_I}}{R_{1I}}\right)\phi_\nu^{AO}(R_I, r) \tag{SI-5}$$

and

$$g_{\mu\nu\kappa\lambda}(R, r) = \int dr_1 dr_2\,\phi_\mu^{AO*}(R_I, r_1)\phi_\nu^{AO*}(R_J, r_2)\frac{e^2}{r_{12}}\phi_\lambda^{AO}(R_K, r_1)\phi_\kappa^{AO}(R_L, r_2) \tag{SI-6}$$

where $R_{1I} = 4\pi\epsilon_0|R_I - r_1|$, and $r_{12} = 4\pi\epsilon_0|r_1 - r_2|$ and $\phi_\mu^{AO}(R_I, r_1)$ is the atomic STO-3G basis function μ of the atom at position R_I and valence charge $\tilde{Z}_I^{s_I}$ (see main text). All integrals are computed using the Gaussian code.[2]

For example, the calculation of the one-body integrals for the 'alchemical' Hamiltonian in a fixed molecular scaffold defined by the N_A coordinates $\{R_I\}$ and N_{SI} possible species for each atom I is given by

$$h_{\mu\nu}^C(\tilde{Z}, R) = -\sum_{\substack{K\neq I\\ L\neq K,I\\ \mu,\nu}}^{N_A,N_A,N_{\mathrm{AO}}^{\mathrm{MAX}}}\sum_{I=1}^{N_A}\sum_{\alpha=1}^{N_{\mathrm{S}}^{\mathrm{MAX}}} Z_I^\alpha\left\langle\phi_\mu^{\mathrm{AO}}(R_K, r)\right|\frac{e^2}{|R_I - r|}\left|\phi_\nu^{\mathrm{AO}}(R_L, r)\right\rangle \tag{SI-7}$$

where $N_{\mathrm{S}}^{\mathrm{MAX}} = \max\{N_{S_1}, \ldots, N_{S_{N_A}}\}$, $\tilde{Z}$ is the ensemble of all $\tilde{Z}_I^{s_I}$, and R the one of all nuclear positions. The classical cost of this operation scales as $\mathcal{O}(N_A^2 N_{AO}^2)\mathcal{O}(N_A)\mathcal{O}(N_{\mathrm{S}}^{\mathrm{MAX}})$. Note that, when the number of valence electrons for the different atoms in the alchemical set (i.e., the pool of atoms used for the alchemical changes) differ, we could enforce for all atoms the same number of valence states (and therefore qubits) using dummy (or empty) orbitals. The algorithm is not therefore confined to iso-electronic elements.

Effective Core Potentials and Active Spaces

To reduce the size of the Hilbert space, effective core potentials (ECPs) are used to replace core electrons in all atoms heavier than H. The use of ECPs allows us to reduce the number of orbitals (and thus qubits) in the calculations. The Gaussian ECP section used for the different atoms are given in Table SI-3.

In the first test case (see Fig.1 of the main text) we used the lowest atomic orbital (i.e., 2 spin orbitals) for each atom in the molecule. While this choice does not guarantee accurate molecular energies (within the so-called chemical accuracy of 1 kcal/mol) it is nonetheless sufficient to provide the correct ranking for the binding energies. The limitation to just 2 basis functions (atomic spin orbitals) is motivated by hardware constraints.

In the second application (see Fig.2 of the main text) we used 8 atomic spin orbitals per atom. This is possible since in this case we only perform simulations of the 'alchemical' quantum algorithm.

Note that in both cases, more accurate results can be achieved using a larger active space (i.e., a larger number of spin orbitals) and better basis sets without changing the nature of the algorithm.

TABLE SI-3. Effective core potentials used to replace the core electrons of the atoms used in our use cases.

Atom	Effective Core Potentials	Atom	Effective Core Potentials	Atom	Effective Core Potential
Li	LI 0 LI-ECP 1 2 p-ul potential 1 1 1.3430600 -0.7306300 s-ul potential 2 0 0.6128400 1.8013100 2 1.6488100 3.5497100	Na	Na 0 Na-ECP 2 10 d-ul potential 5 1 175.5502590 -10.000 2 35.0516791 -47.4902024 2 7.9060270 -17.2283007 2 2.3365719 -6.0637782 2 0.7799867 -0.7299393 s-ul potential 5 0 243.3605846 3.000 1 41.5764759 36.2847626 2 13.2649167 72.9304880 2 3.6797165 23.8401151 2 0.9764209 6.0123861 p-ul potential 6 0 1257.2650682 5.000 1 189.6248810 117.4495683 2 54.5247759 423.3986704 2 13.7449955 109.3247297 2 3.6813579 31.3701656 2 0.9461106 7.1241813	C	C 0 C-ECP 3 2 f potential 1 2 1.00 0.00 s-f potential 1 2 6.401052 33.121638 p-f potential 1 2 7.307747 -1.986257 d-f potential 1 2 5.961796 -9.454318
N	N 0 N-ECP 3 2 f potential 1 2 1.00 0.00 s-f potential 1 2 7.977232 38.533831 p-f potential 1 2 10.183854 -2.550810 d-f potential 1 2 11.559947 -2.995545	O	O 0 O-ECP 3 2 f potential 1 2 1.00 0.00 s-f potential 1 2 10.445670 50.771069 p-f potential 1 2 18.045174 -4.903551 d-f potential 1 2 8.164798 -3.312124	S	S 0 S-ECP 3 10 f potential 1 2 1.00 0.00 s-f potential 1 2 3.743892 37.974819 p-f potential 1 2 3.086088 18.790529 d-f potential 1 2 4.862414 -7.837964

Protein Force Field

The atomic charges of the H-NOX protein (PBD entry code 3TFA) are generated using the Gromacs *pdb2gmx* code and the *gromos54a7.ff* force field with the SPC water model. The original 3TFA.pdb file is made of two units of the same H-NOX protein. In this study, we used the coordinates of the first monomer only. All test molecules (dimers in Table SI-6) are placed with their center of mass at the position of the first co-crystallized Xe atom (the one closer to the protein surface, see Fig.3a of the main text). For the calculation of the binding, we only consider the protein charges within a sphere of radius 11Å from the position of the Xe atom. This radius is chosen such that the total charge of the atoms included is close to zero ($q = 0.12$) to avoid artifacts introduced by the distance cutoff. The corresponding charges in a.u. can be found in Table SI-4.

TABLE SI-4. Charges used to mimic the enzyme pocket. Here we record only the non-zero charges generated by the protein force field calculation.

x	y	z	Charge (a.u.)	x	y	z	Charge (a.u.)	x	y	z	Charge (a.u.)
7.240	21.210	77.100	-0.482	8.480	21.990	78.130	0.241	9.790	14.880	76.560	0.450
10.780	14.800	75.820	-0.450	9.840	14.680	77.870	-0.310	9.010	14.770	78.420	0.310
10.600	15.870	80.470	0.290	11.160	16.820	79.940	-0.450	11.600	12.940	78.080	0.450
12.810	12.770	77.900	-0.450	10.700	11.980	77.880	-0.310	9.740	12.150	78.090	0.310
11.770	10.840	76.000	0.450	12.760	10.180	75.690	-0.450	11.190	11.700	75.170	-0.310
10.390	12.220	75.470	0.310	13.090	12.550	73.840	0.450	13.960	12.200	73.040	-0.450
13.310	13.490	74.750	-0.310	12.560	13.780	75.360	0.310	15.660	13.050	75.310	0.450
16.760	12.950	74.730	-0.450	15.320	12.270	76.330	-0.310	14.440	12.420	76.780	0.310
16.470	10.220	75.670	0.450	17.620	9.820	75.440	-0.450	15.420	9.850	74.960	-0.310
14.510	10.210	75.190	0.310	16.500	9.470	72.770	0.450	17.370	8.740	72.290	-0.450
16.320	10.730	72.370	-0.310	15.600	11.280	72.790	0.310	17.580	13.380	69.940	0.241
17.110	15.060	69.500	-0.482	17.750	15.940	70.930	0.241	18.640	11.350	71.760	0.450
19.540	10.960	71.000	-0.450	18.890	11.810	72.980	-0.310	18.130	12.110	73.550	0.310
20.920	10.530	73.660	0.450	22.130	10.380	73.430	-0.450	20.150	9.530	74.060	-0.310
19.170	9.680	74.220	0.310	19.310	8.150	72.200	0.310	21.020	9.610	70.530	0.310
20.680	10.400	67.530	-0.540	20.840	13.510	68.050	0.140	19.660	12.180	66.890	-0.050
19.020	12.780	66.420	0.310	24.040	13.040	71.530	-0.540	23.810	14.660	70.190	0.140
25.750	14.070	70.610	-0.050	26.300	14.700	70.070	0.310	19.290	12.100	78.880	-0.140
19.970	12.360	78.200	0.140	17.330	11.410	80.810	-0.140	16.640	11.160	81.490	0.140
18.230	12.970	79.190	-0.140	18.170	13.850	78.730	0.140	17.270	12.610	80.150	-0.140
16.530	13.250	80.360	0.140	22.100	15.200	82.480	0.450	21.770	16.250	83.030	-0.450
13.690	12.190	81.750	-0.140	14.550	12.090	81.260	0.140	14.330	13.790	82.910	0.140
13.040	19.690	82.910	0.450	14.190	19.370	82.680	-0.450	12.200	20.100	81.970	-0.310
11.270	20.360	82.230	0.310	11.360	20.450	79.680	0.266	10.370	19.450	79.930	-0.674
9.570	19.620	79.360	0.408	13.670	21.250	80.340	0.450	14.670	20.990	79.670	-0.450
13.480	22.450	80.900	-0.310	12.650	22.620	81.420	0.310	13.010	25.810	79.160	-0.140
13.910	25.700	78.750	0.140	11.970	26.320	78.410	-0.140	12.130	26.590	77.460	0.140
15.860	23.100	81.350	0.450	16.890	23.350	80.730	-0.450	15.860	22.470	82.520	-0.310
15.000	22.300	83.000	0.310	17.800	20.930	82.250	0.450	19.020	20.880	82.160	-0.450
17.000	20.050	81.640	-0.310	16.010	20.090	81.800	0.310	18.230	19.670	79.530	0.450
19.330	19.260	79.160	-0.450	17.570	20.650	78.910	-0.310	16.670	20.910	79.250	0.310
19.440	22.070	78.090	0.450	20.440	21.940	77.380	-0.450	19.450	22.810	79.190	-0.310
18.610	22.910	79.720	0.310	21.820	22.540	79.900	0.450	22.930	22.750	79.420	-0.450
21.560	21.480	80.650	-0.310	20.640	21.370	81.040	0.310	23.090	19.830	79.640	0.450
24.280	19.580	79.500	-0.450	22.190	19.540	78.700	-0.310	21.220	19.720	78.870	0.310
23.490	19.940	76.660	0.450	24.470	19.540	76.040	-0.450	23.150	21.220	76.710	-0.310
22.330	21.500	77.210	0.310	23.330	23.600	76.170	0.266	24.210	24.590	75.650	-0.674
23.780	25.490	75.750	0.408	25.380	22.230	76.600	0.450	26.360	22.230	75.850	-0.450
25.490	22.220	77.920	-0.310	24.670	22.180	78.490	0.310	26.100	19.860	78.910	0.310
27.240	18.680	75.960	-0.310	26.400	19.170	76.220	0.310	27.020	22.320	72.710	-0.310
26.570	21.880	73.480	0.310	26.450	18.660	68.920	0.127	25.690	17.730	68.030	0.129
24.950	17.300	68.560	0.248	25.290	18.250	67.270	0.248	25.230	23.900	72.270	0.450
24.750	23.680	73.380	-0.450	22.590	25.290	72.210	0.450	22.230	24.380	71.460	-0.450
21.840	25.730	73.210	-0.310	22.170	26.480	73.790	0.310	19.650	25.230	72.240	0.450
18.960	24.270	71.900	-0.450	19.690	26.360	71.550	-0.310	20.290	27.100	71.860	0.310
20.600	29.000	71.900	-0.635	19.160	25.550	69.240	0.450	18.260	25.100	68.550	-0.450
20.430	25.200	69.050	-0.310	21.150	25.660	69.570	0.310	24.210	22.740	66.980	0.270
24.620	21.570	66.790	-0.635	20.150	22.820	68.500	0.450	19.650	22.060	67.660	-0.450
20.170	22.520	69.790	-0.310	20.590	23.140	70.450	0.310	18.030	21.310	70.120	0.450
17.410	20.290	69.830	-0.450	17.420	22.480	70.320	-0.310	17.950	23.280	70.600	0.310
15.560	22.290	68.690	0.450	14.590	21.590	68.450	-0.450	16.330	22.810	67.730	-0.310
17.080	23.430	67.990	0.310	16.140	21.000	66.070	0.450	15.210	20.430	65.490	-0.450
17.200	20.340	66.520	-0.310	17.920	20.840	66.990	0.310	16.200	18.160	67.030	0.450
15.660	17.180	66.510	-0.450	15.820	18.630	68.200	-0.310	16.270	19.430	68.590	0.310
13.560	16.480	71.470	-0.140	14.400	15.970	71.300	0.140	12.300	18.500	71.300	-0.140
12.220	19.450	71.000	0.140	12.480	15.850	72.090	-0.140	12.560	14.890	72.370	0.140
11.210	17.880	71.920	-0.140	10.370	18.400	72.080	0.140	11.300	16.550	72.320	-0.140
10.530	16.110	72.770	0.140	13.380	18.140	68.230	0.450	12.600	17.200	68.190	-0.450
13.110	19.320	67.690	-0.310	13.760	20.070	67.780	0.310	11.740	18.590	65.780	0.450
10.680	18.040	65.500	-0.450	12.840	18.390	65.080	-0.310	13.680	18.890	65.310	0.310
12.600	16.010	64.460	0.450	13.240	15.640	65.560	-0.310	13.810	16.310	66.040	0.310
15.180	11.920	67.230	-0.140	15.690	12.230	66.430	0.140	13.570	12.340	68.940	-0.140
12.930	12.950	69.400	0.140	15.380	10.640	67.720	-0.140	16.040	10.040	67.280	0.140
13.760	11.050	69.430	-0.140	13.230	10.740	70.230	0.140	14.670	10.210	68.820	0.203
14.870	8.920	69.290	-0.611	14.280	8.760	70.090	0.408	11.700	13.960	66.540	0.450
11.010	14.960	67.070	-0.310	11.420	15.870	67.070	0.310	7.840	16.080	68.860	-0.210
8.230	14.830	71.110	-0.140	9.210	14.650	70.980	0.140	7.580	14.410	72.250	-0.140
8.090	13.920	72.960	0.140	13.170	28.290	72.750	-0.450	13.360	25.750	67.330	0.450
13.620	25.100	66.320	-0.450	12.630	25.260	68.330	-0.310	12.490	25.800	69.160	0.310
10.920	22.050	69.540	0.241	10.210	21.610	71.140	-0.482	8.630	22.440	71.030	0.241
10.960	23.910	67.090	0.450	10.850	22.920	66.360	-0.450				

Reference binding Energies from classical calculations

To validate results of our 'alchemical' optimizations, we performed classical quantum chemistry calculations of all possible structures (still affordable due to the limited number of atomic sites and atomic species considered in these proof-of-principle study) using Gaussian.[2] Molecules that would bind in a given point charge environment show negative binding energies. Positive values indicate that the molecules have no affinity for the binding site.

The results for the binding energies are summarized in Tables SI-5 (for the fist test system described in Fig. 1 of the main text) and SI-6 (for the second test case in Fig.3) and confirm the correctness of the 'alchemical' predictions obtained using the proposed quantum algorithm.

TABLE SI-5. Binding Energies for the different diatomic molecular structures for the three different charges environments calculated in the full active space using Gaussian code.[2] Energies are computed at CCSD level of accuracy.

Atomic Composition	Binding Energies (mHartree)		
	Case1	Case2	Case 3
H_2	-0.62948	-1.10845	-0.41422
HLi	-4.23166	30.00577	1.431840
HNa	-2.02120	50.65077	4.247418
LiH	-4.23166	-39.8559	-5.59603
Li_2	**-9.72620**	-33.8006	-1.43048
LiNa	-9.32586	31.42160	5.535703
NaH	-2.02120	-57.5656	**-6.62025**
NaLi	-9.32586	**-80.7604**	-5.98487
Na_2	-5.00948	-27.1735	-1.33592

TABLE SI-6. Binding energies and Force Field Calculations for diatomic molecular structures within the protein environment. Binding energies are calculated within the full active space with the Gaussian code.[2]The self energy of the charges introduced to mimic the enzyme pocket is -6.3667 a.u. for all cases.

Atomic Composition	Binding Energies(mHartree)		
	CCSD	B3LYP	Force Field
CN	-0.5479	-0.3264	-0.3745
OC	-0.3134	-0.0848	0.4468
ON	-0.4147	-0.1971	0.1056
SC	-0.6329	-0.4491	-0.5136
SN	-1.0435	-0.8188	-0.7700
SO	**-1.1684**	**-1.0922**	**-0.8313**

Interpretation of the statistical outcome

In the case outcome of the alchemical optimization consists in an ensemble of structures with similar weights, this can be taken as an opportunity since it offers us the possibility to choose from the pool of candidates the structure that fulfills additional conditions that are hard to encode in a cost function such as: stability, possibility of synthesis, and production costs, just to mention a few. After all, in molecular design we are not necessarily interested in the absolute best possible molecule, but we aim at a list of valid candidates to propose for synthesis. On the other hand, if this uncertainty is constituting a problem in future applications, we can also trivially modify our algorithm and include a penalty term in the cost function that penalizes distributions of weights (i.e., the coefficients α) with many non-zero terms, e.g., by using L1-regularization very common in classical machine learning. In this case, the outcome of our algorithm will only consist of a small number of 'optimal' structures.

Description of the Quantum Hardware

The calculations are performed using the 20 qubit processor *ibmq_singapore*. The connectivity of the hardware is shown in Fig. SI-1. For the calculations we used 4 out of the 20 available qubits, namely qubits labelled as 0,1,2 and 3. The operating frequencies of the qubits range from 4.67 to 4.78 GHz and the average coherence and relaxation times of the qubits are about 89.5 and 133 mus, respectively.

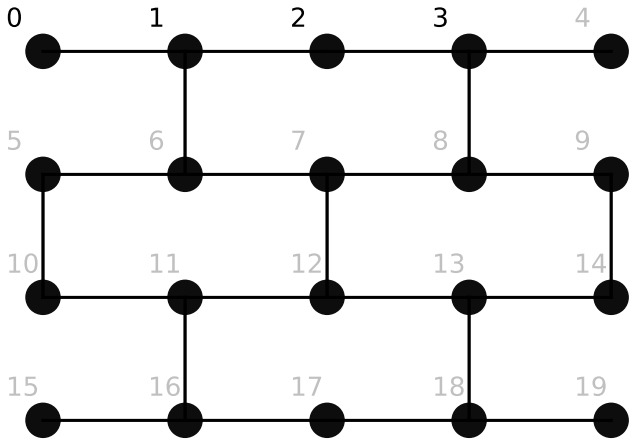

FIG. SI-1. Connectivity of the *ibmq_singapore* chip. The qubits used are qubits 0,1,2 and 3 with their natural connectivity. Hardware access and data provided via Qiskit[3]

---

[1] *NIST Computational Chemistry Comparison and Benchmark Database; NIST Standard Reference Database Number 101; http://cccbdb.nist.gov/.*

[2] M. J. Frisch, G. W. Trucks, H. B. Schlegel, G. E. Scuseria, M. A. Robb, J. R. Cheeseman, G. Scalmani, V. Barone, G. A. Petersson, H. Nakatsuji, X. Li, M. Caricato, A. V. Marenich, J. Bloino, B. G. Janesko, R. Gomperts, B. Mennucci, H. P. Hratchian, J. V. Ortiz, A. F. Izmaylov, J. L. Sonnenberg, D. Williams-Young, F. Ding, F. Lipparini, F. Egidi, J. Goings, B. Peng, A. Petrone, T. Henderson, D. Ranasinghe, V. G. Zakrzewski, J. Gao, N. Rega, G. Zheng, W. Liang, M. Hada, M. Ehara, K. Toyota, R. Fukuda, J. Hasegawa, M. Ishida, T. Nakajima, Y. Honda, O. Kitao, H. Nakai, T. Vreven, K. Throssell, J. A. Montgomery, Jr., J. E. Peralta, F. Ogliaro, M. J. Bearpark, J. J. Heyd, E. N. Brothers, K. N. Kudin, V. N. Staroverov, T. A. Keith, R. Kobayashi, J. Normand, K. Raghavachari, A. P. Rendell, J. C. Burant, S. S. Iyengar, J. Tomasi, M. Cossi, J. M. Millam, M. Klene, C. Adamo, R. Cammi, J. W. Ochterski, R. L. Martin, K. Morokuma, O. Farkas, J. B. Foresman, and D. J. Fox, "Gaussian 16 Revision C.01," (2016), gaussian Inc. Wallingford CT.

[3] G. Aleksandrowicz, T. Alexander, P. Barkoutsos, L. Bello, Y. Ben-Haim, D. Bucher, F. J. Cabrera-Hernández, J. Carballo-Franquis, A. Chen, C.-F. Chen, J. M. Chow, A. D. Córcoles-Gonzales, A. J. Cross, A. Cross, J. Cruz-Benito, C. Culver, S. D. L. P. González, E. D. L. Torre, D. Ding, E. Dumitrescu, I. Duran, P. Eendebak, M. Everitt, I. F. Sertage, A. Frisch, A. Fuhrer, J. Gambetta, B. G. Gago, J. Gomez-Mosquera, D. Greenberg, I. Hamamura, V. Havlicek, J. Hellmers, Ł. Herok, H. Horii, S. Hu, T. Imamichi, T. Itoko, A. Javadi-Abhari, N. Kanazawa, A. Karazeev, K. Krsulich, P. Liu, Y. Luh, Y. Maeng, M. Marques, F. J. Martín-Fernández, D. T. McClure, D. McKay, S. Meesala, A. Mezzacapo, N. Moll, D. M. Rodríguez, G. Nannicini, P. Nation, P. Ollitrault, L. J. O'Riordan, H. Paik, J. Pérez, A. Phan, M. Pistoia, V. Prutyanov, M. Reuter, J. Rice, A. R. Davila, R. H. P. Rudy, M. Ryu, N. Sathaye, C. Schnabel, E. Schoute, K. Setia, Y. Shi, A. Silva, Y. Siraichi, S. Sivarajah, J. A. Smolin, M. Soeken, H. Takahashi, I. Tavernelli, C. Taylor, P. Taylour, K. Trabing, M. Treinish, W. Turner, D. Vogt-Lee, C. Vuillot, J. A. Wildstrom, J. Wilson, E. Winston, C. Wood, S. Wood, S. Wörner, I. Y. Akhalwaya, and C. Zoufal, "Qiskit: An open-source framework for quantum computing" (2019).